Masthead Logo

Journal of Geospatial Applications in Natural Resources

Volume 1 | Issue 1 Article 1

1-13-2016

Comparison of Terrain Indices and Landform Classification Procedures in Low-Relief Agricultural Fields

Derek A. Evans
derekae88@gmail.com

Karl W. J. Williard
Southern Illinois University Carbondale, williard@siu.edu

Jon E. Schoonover
jschoon@siu.edu

Journal of Geospatial Applications in Natural Resources Vol. 1, No. 1; 2016

Comparison of Terrain Indices and Landform Classification Procedures in Low-Relief Agricultural Fields

Derek A. Evans[1], Karl W. J. Williard[2], and Jon E. Schoonover[2]

[1]Information Technology Services, University of Tennessee Institute of Agriculture, Knoxville, Tennessee, USA

[2]Department of Forestry, Southern Illinois University, Carbondale, Illinois, USA

Correspondence: Derek A. Evans, Information Technology Services, University of Tennessee Institute of Agriculture, Knoxville, Tennessee, USA. E-mail: derekae88@gmail.com.

Received: October 24, 2015 Accepted: December 15, 2015 Published: January 13, 2016

Abstract

Landforms control the spatial distribution of numerous factors associated with agronomy and water quality. Although curvature and slope are the fundamental surface derivatives used in landform classification procedures, methodologies for landform classifications have been performed with other terrain indices including the topographic position index (TPI) and the convergence index (CI). The objectives of this study are to compare plan curvature, the convergence index, profile curvature, and the topographic position index at various scales to determine which better identifies the spatial variability of soil phosphorus (P) within three low relief agricultural fields in central Illinois and to compare how two methods of landform classification, e.g. Pennock et al. (1987) and a modified approach to the TPI method (Weiss 2001, Jenness 2006), capture the variability of spatial soil P within an agricultural field. Soil sampling was performed on a 0.4 ha grid within three agricultural fields located near Decatur, IL and samples were analyzed for Mehlich-3 phosphorus. A 10-m DEM of the three fields was also generated from a survey performed with a real time kinematic global positioning system. The DEM was used to generate rasters of profile curvature, plan curvature, topographic position index, and convergence index in each of the three fields at scales ranging from 10 m to 150 m radii. In two of the three study sites, the TPI ($r \geq -0.42$) was better correlated to soil P than profile curvature ($r \leq 0.41$), while the CI ($r \geq -0.52$) was better correlated to soil P than plan curvature ($r \geq -0.45$) in all three sites. Although the Pennock method of landform classification failed to identify footslopes and shoulders, which are clearly part of these fields' topographic framework, the Pennock method ($R^2 = 0.29$) and TPI method ($R^2 = 0.30$) classified landforms that captured similar amounts of soil P spatial variability in two of the three study sites. The TPI and CI should be further explored when performing terrain analysis at the agricultural field scale to create solutions for precision management objectives.

Keywords: Landform classification, topographic position index, convergence index, curvature, scale, GIS

Introduction

Landforms control the spatial distribution of numerous factors associated with agronomy and water quality, including soil water distribution (Hawley et al. 1983), surface runoff generation (Needleman et al. 2004), soil nutrients typically amended through fertilization (Soon and Malhi 2005, Balkcom et al. 2005, Brubaker et al. 1993),

and crop yields (Kravchenko and Bullock 2000). Although various procedures for classifying landforms exist (Dikau 1989, Pennock et al. 1987, Schmidt and Hewitt 2004), curvature and slope are the fundamental surface derivatives used in classification procedures because they describe the geometric form of the landscape at any given point (Schmidt and Hewitt 2004). These geometric forms, e.g. convex, concave, planar, convergent, and divergent, characterize topographic factors that control overland and intrasoil water flow convergence/divergence and acceleration/deceleration which, ultimately, influence the spatial distribution of soil properties (Kirkby and Chorley 1967, Florinsky 2012).

Considering that various landscape processes dominate at various scales (Florinsky and Kuryakova 2000), scale is integrated into terrain attribute derivations to better capture topographic influence on soil parameter(s). The adequate scale for analysis must be found relative to the dataset and the purpose of the study (Dragut et al. 2009). Scale has been incorporated in previous research by increasing DEM cell size (Florinsky and Kuryakova 2000), filtering surface derivatives calculated by the standard three by three cell neighborhood size of a DEM through focal mean statistics with varying neighborhood sizes (Dragut et al. 2009), and fitting a quadratic trend surface to a *n* by *n* cell neighborhood through least squares (Wood 1996). To determine which scale to use for delineating topographic position, terrain attributes calculated at multiple scales are correlated to soil parameter(s) of interest and correlations are plotted against each scale. Areas of the graph that exhibit smooth variations and statistically significant correlations indicate ranges of adequate scales that should be considered for further analysis of the soil parameter(s) (Florinsky and Kuryakova 2000). Areas on the same graph where soil parameter and scaled surface derivatives peak have also been used in determining adequate scale (Dragut et al. 2009).

Although surface derivatives are primarily used to describe terrain geometries and classify landforms, methodologies for landform classifications have been performed with other terrain indices. The topographic position index (TPI) method of landform classification has been applied across numerous disciplines since Jenness (2006) created the Topographic Position Index and Slope Position Classification (SPC) tool for ArcGIS (ESRI, Redlands, CA) (De Reu et al. 2013). Soil predictive mapping investigations have utilized the TPI method and were able to spatially predict soil units with up to 70% accuracy (Deumlich et al. 2010). The convergence index (CI) represents the agreement of a cell's surrounding neighbors' aspect to a theoretical maximum convergent direction matrix. The CI is applicable as a valley recognition tool as well as for analysis of channel/ridge systems (GRASS Development Team, 2015). The CI has been used in delineating thalweg networks in a badlands landscape where it outperformed plan curvature (Thommeret et al. 2010).

Farm managers today are adopting precision agriculture technologies to increase the profitability of agricultural operations by identifying within field soil variabilities and managing them based on crop productivity potential. Tools and technologies present within precision agriculture have allowed farm managers to collect highly accurate spatial datasets at the agricultural field scale. Among these spatial datasets are DEMs. With the DEM, topographic indices can be generated that help describe the geometric form of the landscape as well as delineate landform elements. Since landform elements control the spatial distribution of soil properties critical to agronomic factors, the characterization of DEMs into landform units can provide zones that capture the variability of agronomic factors.

Journal of Geospatial Applications in Natural Resources Vol. 1, No. 1; 2016

Objectives

The objectives of this study are to 1) compare two terrain indices that pertain to flow convergence/divergence, e.g. plan curvature and CI, and two terrain indices that pertain to slope position and flow acceleration/deceleration, e.g. profile curvature and TPI, to determine which better identifies the spatial variability of soil phosphorus (P) within three low relief agricultural fields in central Illinois, 2) identify appropriate scales for deriving topographic indices, and 3) compare how two methods of landform classification, e.g. Pennock et al. (1987) and TPI method, capture the variability of spatial soil P within an agricultural field. Soil P was chosen for this study because soil P is spatially driven by landform elements (Kravchenko and Bullock 2000, Brubaker et al. 1994, Malo and Worcester 1974), soil P is commonly amended in agriculture through fertilization, and soil P is commonly analyzed for agronomic purposes. Landforms were classified according to Pennock et al. (1987) descriptions. Identifying the proper scales for deriving terrain indices as well as defining a suitable method for landform classification in a low relief agricultural field can help farm managers better utilize DEM data for precision management.

Methods

Study Sites

The study sites are three agricultural fields (BRKA9, BRKA10, and BRKA11) that are part of a paired watershed study located near Decatur, IL (Figure 1). The three fields are located directly adjacent to one another and each

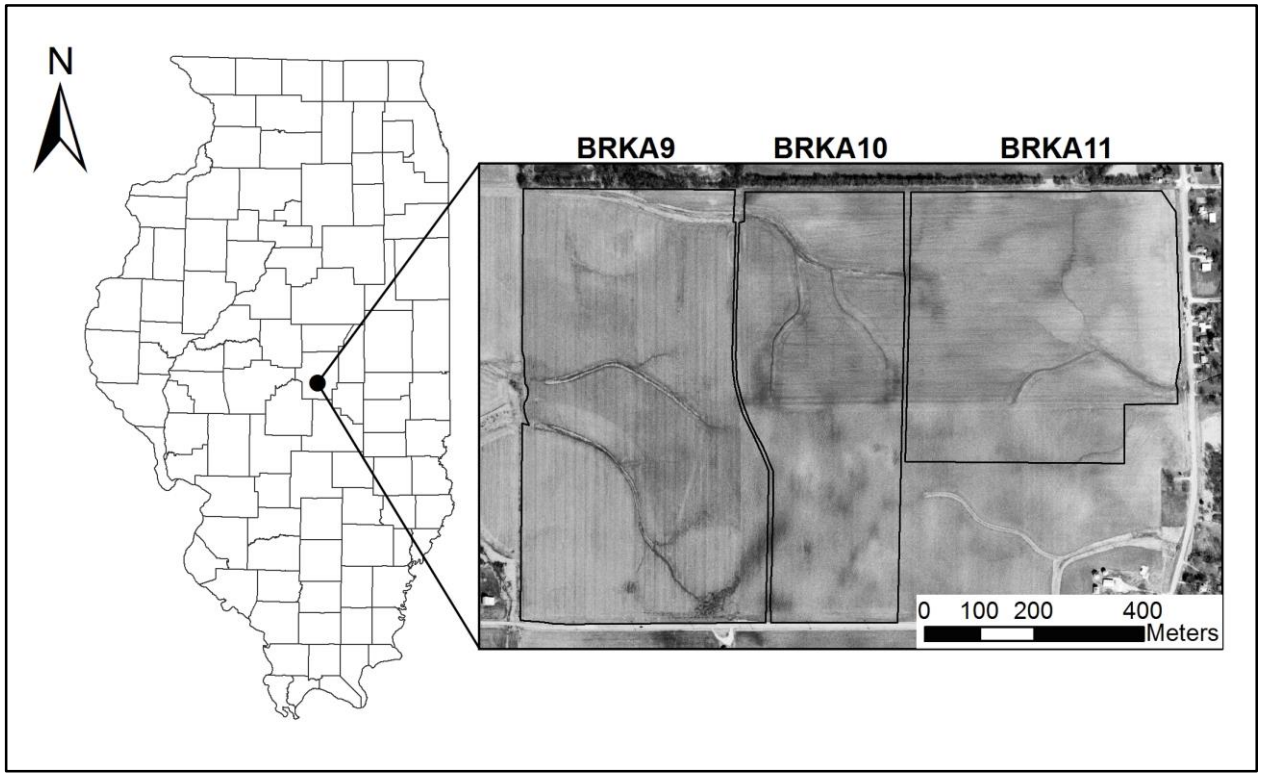

Figure 1. Study sites located approximately 5km south of Decatur, IL. Aerial imagery was taken in 2005 and was retrieved from the Illinois State Geological Survey Geospatial Data Clearinghouse (http://clearinghouse.isgs.illinois.edu/).

Table 1. Fertilizer application dates and rates applied at BRKA9, BRKA10, and BRKA11.

Field	Date Applied	Fertilizer	Rate
BRKA9	4/12/2010	Potash	365.1 kg ha^{-1}†
	11/1/2010	DAP‡	392 kg ha^{-1}
	11/4/2010	Anhydrous	187.04 kg ha^{-1}
	11/4/2010	N-Serve	2.3 kg L^{-1}
	11/3/2010	Lime	1792 kg ha^{-1}†
BRKA10	4/12/2010	Potash	243.0 kg ha^{-1}†
	11/1/2010	DAP	366.24 kg ha^{-1}†
	11/4/2010	Anhydrous	192.59 kg ha^{-1}†
	11/4/2010	N-Serve	2.3 kg L^{-1}
	11/3/2010	Lime	4480 kg ha^{-1}†
BRKA11	4/11/2010	Potash	300.2 kg ha^{-1}†
	11/1/2010	DAP	321.44 kg ha^{-1}†
	11/4/2010	Anhydrous	203.51 kg ha^{-1}†
	11/4/2010	N-Serve	2.3 kg L^{-1}
	11/3/2010	Lime	2240 kg ha^{-1}†

†Applied at a variable rate – rates shown are averages.

‡DAP, diammonium phosphate

field contains one experimental watershed. BRKA9, BRKA10, and BRKA11 were soybeans (*Glycine Max* (L.) Merr.) in 2010 and corn (*Zea mays* L.) in 2011. The fields have been under no-till management since 2010 and received fertilizer applications based on individual field soil sampling test values. Fertilizer application rates for 2010 and 2011 are shown in Table 1. BRKA9, BRKA10, and BRKA11 are located within the Bloomington Ridged Plain physiographic division which contains most of the Wisconsin moraines. The Bloomington Ridged Plain is characterized as relatively flat or gently undulating (Collman 2009). BRKA9 is 32.9 ha and consists mainly of 0-2% slopes with 5-10% slopes occurring in its northwest corner. Rills and grass waterways drain water to the eastern edge of the field. The relief of BRKA9 is 10m. BRKA10 is 21.4 ha with 7 m of relief. A level (<1% slope), upland region is located in the southern half of BRKA10. Grass waterways located on a gradual (0-2% slope) hillslope drain water from the field; 2-5% slopes occur on the northern edge and southeastern corner of BRKA10. BRKA11 is 23.3 ha and consists mainly of 0-2% slopes; 5-10% slopes occur in the northeastern corner of the field while 2-5% slopes occur on the eastern edge and southeastern corner. An upland region is located on the western edge of BRKA11 and water drains from the west to the east within large rills and grass waterways. The relief of BRKA11 is 10 m.

The dominant soil series within the three fields are Flannigan silt loam (Fine, smectitic, mesic Aquic Argiudolls), Drummer silty clay loam (Fine-silty, mixed, superactive, mesic Typic Endoaquolls), and Wingate silt loam (Fine-silty, mixed, superactive, mesic Mollic Oxyaquic Hapludalfs). The Flannigan soil series is somewhat poorly

drained and slightly acidic, spatially occurring on convex areas with a typical slope of 0-4%. The Drummer soil series is poorly drained and moderately acidic, spatially occurring on level areas or depressions with 0-2% slope. The Drummer soil series is geographically associated with Flannigan soil series by forming the drainage network that drains water from upslope landform position where the Flannigan soil series occurs. The Wingate soil series is moderately well drained and neutral, occurring on convex areas with 0-10% slopes (Soil Survey Staff, NRCS, USDA).

Digital Elevation Model

A 10-m digital elevation model (DEM) was created for BRKA9, BRKA10, and BRKA11 (Figure 2) from a survey taken with a real time kinematic global positioning system (John Deere Starfire, Deere & Company, Moline, Illinois) mounted on an ATV. Elevation data were logged at a one second interval in transects spaced 4.6 meters apart within each field. Delaunay triangulation was used to interpolate the elevation point data for each field. The triangulated surfaces were then converted to a 10-m raster through linear interpolation of the triangles using the 3D Analyst extension in ArcGIS (ESRI, Redlands, CA). To remove noise in the DEM surfaces, a low pass filter was applied and sinks were filled in the filtered DEM using the Spatial Analyst extension in ArcGIS. Although

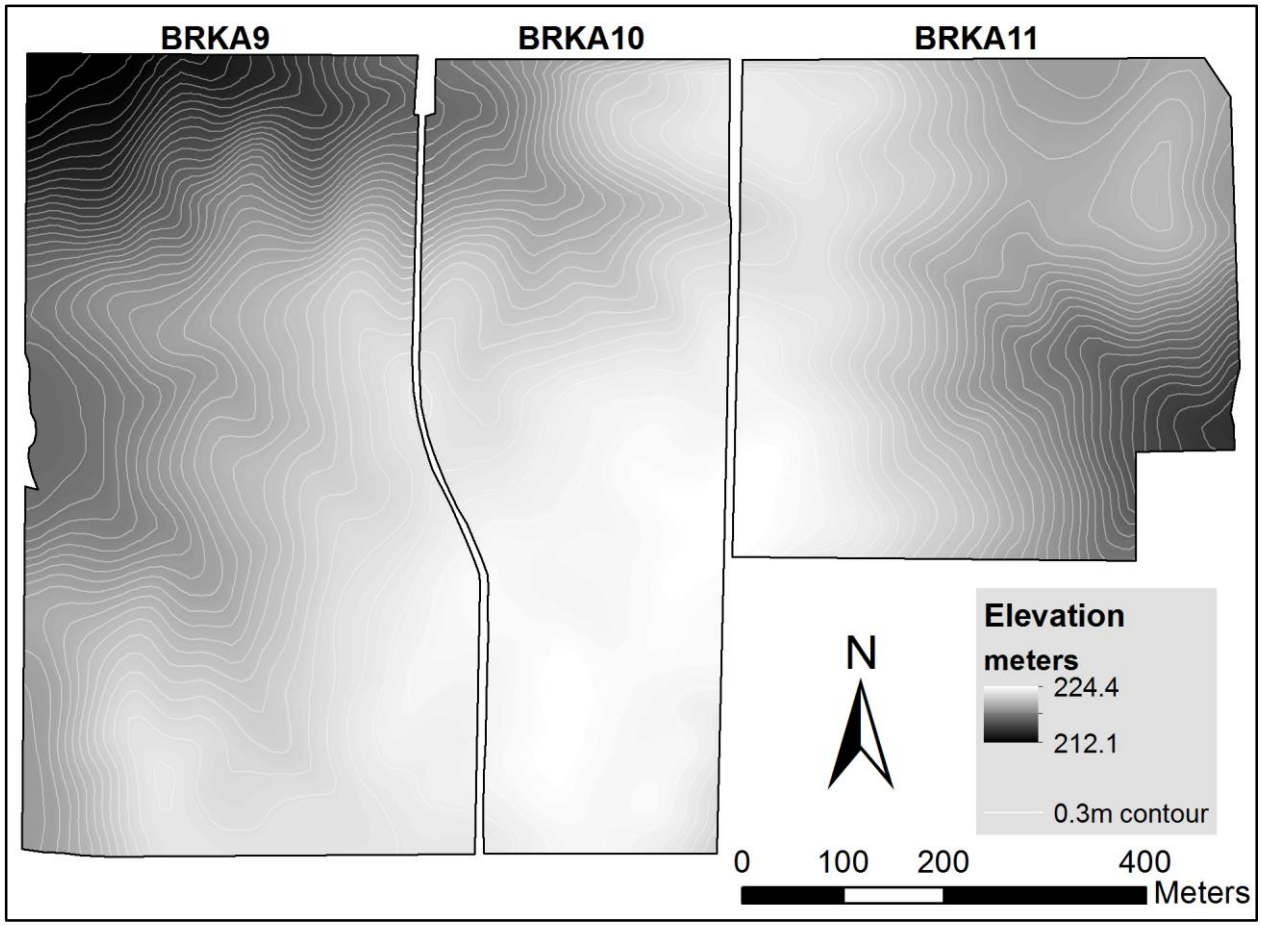

Figure 2. The 10-m digital elevation model of BRKA9, BRKA10, and BRKA11.

BRKA9, BRKA10, and BRKA11 are located directly adjacent to one another, DEMs for each field were generated from georeferenced elevation data taken within each field only because each field is treated as an individual management and experimental unit. Subsequent terrain analysis is performed on each individual DEM generated for each field.

Soil Sampling

Soil sampling was done on a 0.4 ha grid in October 2011 at BRKA9 (n = 77), BRKA10 (n=55), and BRKA11 (n=60) on the same day. One composite soil sample consisting of six 15 cm long by 1.91 cm diameter soil cores was taken every 0.4 ha. Samples were air-dried, ground by a Dynacrush soil grinder (Custom Laboratory Equipment Inc., Orange City, FL) to pass through a 2mm mesh screen, and analyzed by Brookside Laboratories, Inc., (New Knoxville, OH) for Mehlich-3 P (Mehlich 1984). Soil results were interpolated through inverse distance weighting with a power of two using ArcGIS Geostatistical Analyst.

Topographic Indices

Both plan curvature and profile curvature are used extensively for landform classification procedures (Pennock et al. 1987, Dikau 1989, Burrough et al. 2000, Dragut and Blaschke 2006). Plan and profile curvature control divergence/convergence and acceleration/deceleration, respectively, of gravity driven flow (Florinsky 2012). Plan and profile curvature are both second derivatives of the elevation surface; plan curvature measures the rate of change along a contour while profile curvature measures the rate of change parallel to the slope. Curvature is calculated from the coefficients of the polynomial used to model the elevation surface. Plan and profile surfaces were derived on a 3×3 plane square-gridded window with ArcGIS. Positive and negative plan curvature values indicate a convex and concave surface, respectively. Positive and negative profile curvature values indicate a concave and convex surface, respectively. Plan and profile surfaces that are approximately zero are considered linear. Plan and profile curvature rasters were scaled by taking a focal mean of neighborhood cells within a circular neighborhood (Deng et al. 2007, Dragut et al. 2009). Focal means were calculated with the Focal Statistics tool in ArcGIS. The radius of the circular neighborhood determined the scale at which plan and profile curvature was derived. A circular neighborhood removes the directional bias associated with square neighborhoods – neighborhood edge cells located directly north, south, east, and west from the center of the neighborhood are closer than all other cells. Edge cells in a circular neighborhood are all equidistant from the center of the neighborhood. Also, Shi et al. (2007) found that circular neighborhoods outperform square neighborhoods when deriving slope gradient of a DEM. Neighborhood radii (NR) ranging from 10-150 m were used to simulate plan and profile curvature scales. Focal mean plan and profile curvature rasters were generated at 10-m increments, producing 15 rasters representing 15 differing scales for both plan and profile curvature.

The TPI is the difference of a cell elevation (e) in a digital elevation model (DEM) from the mean elevation (μ_e) of a user specified neighborhood surrounding and also including e. If TPI ≈ 0, the cell is either on a level plane or on a plane with nearly equal slope, e.g. backslope. If TPI > 0, the cell is at a location higher than the mean elevation of its surroundings, e.g. shoulder. If TPI < 0, the cell is at a location lower than the mean elevation of its surroundings, e.g. footslope. A circular neighborhood was used to calculate TPI of the BRKA DEM at NR ranging from 10 m – 150 m in 10-m increments in ArcGIS.

The convergence index (CI) is a measure of convergence, divergence, and planarity. The CI is calculated as the mean difference between the real slope direction or aspect of cells within a neighborhood and the direction to the neighborhood's center cell minus 90 degrees. The CI ranges from -90 degrees (maximum convergence) to 90 degrees (maximum divergence). The System for Automated Geoscientific Analyses (SAGA) was used to calculate the CI of the BRKA DEM at NR ranging from 10 m – 150m in 10-m increments. SAGA scaled the CI to range from -100 and 100.

To determine the appropriate scale for deriving each terrain indices, an approach similar to Florinsky and Kuryakova (2000) and Dragut et al. (2009) was adopted. NR where correlation between soil P and topographic indices peaked were deemed the most suitable scales for deriving the individual terrain indices.

Landform Classification

Two methods were used to delineate landforms at BRKA with the four terrain indices derived at scales found most appropriate for influencing soil P spatial distribution. The first method was that described by Pennock et al. (1987). This method incorporates plan and profile curvature to delineate convergent/divergent footslopes, backslopes, shoulders, and level areas. Profile curvature <-0.10°/m identified footslopes (concave), profile curvature >0.10°/m identified shoulders (convex), and -0.10 °/m<profile curvature<0.10°/m identified linear areas. Considering that ArcGIS outputs profile rasters were concave surfaces are expressed as positive values and convex surfaces are expressed as negative values, profile curvature outputs were multiplied by negative one to match Pennock descriptions. Although Pennock et al. (1987) used 5% slope (3°) to classify linear areas into backslopes and level areas, a slope threshold of <1% was chosen to represent level areas because it was assumed that linear areas with slopes <1% would not produce contributing surface runoff to downslope topographic positions. These areas are most likely sinks or depositional areas. Also, sheet erosion has been known to occur on slopes as little as 1% (Pimentel 2000). Slope was calculated at the same scale as the profile curvature raster that best correlated with soil P since slope was used to differentiate between slope positions classified with profile curvature only. The same method used to scale curvature was used to scale slope. Further, areas with plan curvature < 0 were convergent whereas areas with plan curvature > 0 were divergent areas.

The second method was a modification of the TPI method. Weiss (2001) and Jenness (2006) recommend standard deviations (σ_{TPI}) away from the mean TPI raster (μ_{TPI}) as threshold values for classifying six slope positions: valley ($TPI < \mu_{TPI} - \sigma_{TPI}$), lower slope ($\mu_{TPI} - \sigma_{TPI} \leq TPI < \mu_{TPI} - 0.5\sigma_{TPI}$), middle slope ($\mu_{TPI} - 0.5\sigma_{TPI} \leq TPI \leq \mu_{TPI} + 0.5\sigma_{TPI}$; slope>5°), flat area ($(\mu_{TPI} - 0.5\sigma_{TPI} \leq TPI \leq \mu_{TPI} + 0.5\sigma_{TPI}$; slope≤5°), upper slope ($\mu_{TPI} + 0.5\sigma_{TPI} < TPI \leq \mu_{TPI} + \sigma_{TPI}$), and ridge ($TPI > \mu_{TPI} + \sigma_{TPI}$). To remain consistent with Pennock et al. (1987) descriptions, $TPI < \mu_{TPI} - 0.75\sigma_{TPI}$ identified footslopes, $TPI > \mu_{TPI} + 0.75\sigma_{TPI}$ identified shoulders, and $\mu_{TPI} - 0.75\sigma_{TPI} < TPI < \mu_{TPI} + 0.75\sigma_{TPI}$ identified linear areas, e.g. backslopes and level areas. To separate between backslopes and level areas, a slope threshold of <1% was chosen for aforementioned reasons. Slope was calculated at the scale in which TPI was derived since it was used to differentiate between slope positions classified with TPI only. Convergence/divergence of footslope, backslopes, and shoulders was determined by the CI: CI<0 was convergent and CI>0 was divergent.

Statistical Analysis

The PROC CORR command in SAS was used to conduct a Pearson's correlation (*r*) between TPI, CI, plan

curvature, and profile curvature derived at various scales and soil P. Soil P data was log transformed to normalize the data. The PROC GLM command in the statistical analysis software SAS (SAS Institute Inc., Cary, NC) was used to conduct a fixed effects one-way ANOVA on soil nutrient data by each methods' landform classifications and also to calculate the percent variability explained (R^2) in soil P. The R^2 was calculated as the ratio of the between group sum of squares and the total sum of squares. Observations that were ± 2 standard deviations away from group means were considered outliers and removed from analysis. The data was also log transformed to meet normality and equality of variance assumptions. Further, multiple comparisons were made between groups with the Tukey procedure. Statistical significance for all tests was set at $\alpha = 0.05$.

Results

Soil Phosphorus

Soil P mean±standard error for BRKA9 was 40.6±2.2 mg kg^{-1}. BRKA9 soil P levels tended to be higher in areas where multiple rills converge into the southern-most waterway and at the outlet were both the southern and central waterways converge at the western edge of the field (Figure 3). Soil P tended to be higher in upper reaches of the watersheds that are drained by the southern and central waterway. Soil P also appears to accumulate at the base of slopes in the northern edge of the field near the waterway. Lower soil P concentrations were associated with areas of larger percent slope, such as in the northern and southwestern portions of the field.

BRKA10 soil P accumulated at the northwest outlet where all grass waterways in the field drain (Fig. 3). Soil P in BRKA10 also accumulated in convergent areas located near grass waterways and convergent areas located in the flat, upland region that is characteristic of the southern half of the field. Divergent areas of BRKA10 appear to be lowest in soil P. Soil P mean±standard error for BRKA10 was 59.0±4.0 mg kg^{-1}.

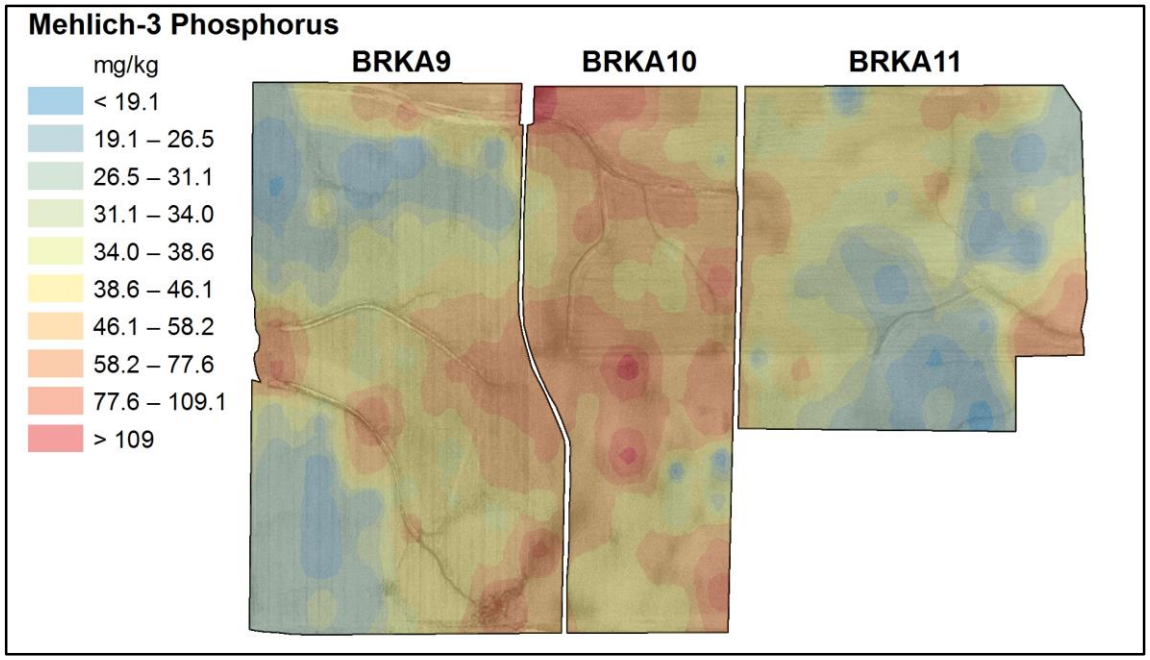

Figure 3. Soil phosphorus distribution throughout BRKA9, BRKA10, and BRKA11.

Journal of Geospatial Applications in Natural Resources Vol. 1, No. 1; 2016

Much like BRKA9 and BRKA10, BRKA11 had higher levels of soil P that accumulated at the outlet where most flow drains (Figure 3). Convergent areas on the western and northern edge of BRKA11 were also higher in soil P. The upland area on the western edge of the field contained moderate levels of soil P while areas with higher percent slope contained lower soil P. A divergent area on the northeast portion of the field was also lower in soil P. Soil P mean±standard error for BRKA10 was 36.4±2.0 mg kg^{-1}.

The spatial distribution of soil P within all three fields suggests that slope and surface runoff convergence/divergence and acceleration/deceleration plays a major role in P mobility. Outlets of rills and grass waterways accumulate soil P from upslope positions where surface runoff erodes soil and deposits particulate bound P at the catchment outlet. This suggests that the catchment outlets both converge and decelerate surface runoff, allowing for particulate phosphorus bound to suspended sediment to settle. Further, upslope and downslope areas typically had more soil P than midslope areas, especially in BRKA9 and BRKA11. These midslope areas have greater slopes which accelerate surface runoff and erode soil P depositing it in downslope positions. Upslope positions generally contain larger soil P because surface runoff either does not occur or occurs at much lower velocities that cause less erosion compared to midslopes. As seen in Figure 3, BRKA10 has more soil P situated along flow accumulating areas than in areas where flow diverges. The lower slope of BRKA10 compared to BRKA9 and BRKA11 allowed the convergence and divergence of surface runoff to dominate soil P distribution.

Spatial variations of soil P could also be caused by soil variabilities associated with the dominant soil series throughout the study sites. In acidic soils such as the Flanagan and Drummer soil series, inorganic soil P may become fixed to iron oxides. During periods of anaerobic conditions, iron reduction causes the iron-phosphate complex to become soluble, releasing P to the soil solution (Havlin et al., 2005). Since the Flanagan and Drummer soil series are somewhat poorly and poorly drained, respectively, soil P availability could potential be greater in these soils than the Wingate soil series, especially after a saturating rainfall. This phenomenon could have implications for the higher concentrations of soil P in BRKA10. Further, P fixation is greater in soils with a higher fraction of finer particles, e.g. clay, suggesting that the Drummer soil series would have a greater phosphorus fixing capacity than the Flanagan and Wingate soil series (Hansen et al. 2002). Since soil P is generally greater in the drainage network where the Drummer series is located, it is possible that the P fixation sites are saturated or near saturation causing soil P additions from upslope sources and fertilizer P to remain in the soil solution (Havlin et al. 2005). This could also explain the soil P "hot spots" situated along the waterways where multiple rills converge and at the watershed outlets.

Scale

Peaks in *r* between each scaled terrain index and soil P occurred at various NR for each field (Figure 4). Peak *r* for plan curvature, CI, and TPI in BRKA9 occurred at a scale of 40m while the peak *r* for profile curvature occurred at 10 m (Figure 5). CI had the greatest correlation with soil P ($r=-0.52$, $p<0.001$) in BRKA9. Convergent/divergent terrain indices were better correlated with soil P than acceleration/deceleration terrain indices indicating that soil P spatial distribution is affected more by flow convergence/divergence. Further, CI performed better than plan curvature ($r=-0.45$, $p<0.001$) while TPI ($r=-0.42$, $p<0.001$) performed better than profile curvature ($r=0.28$, $p<0.05$).

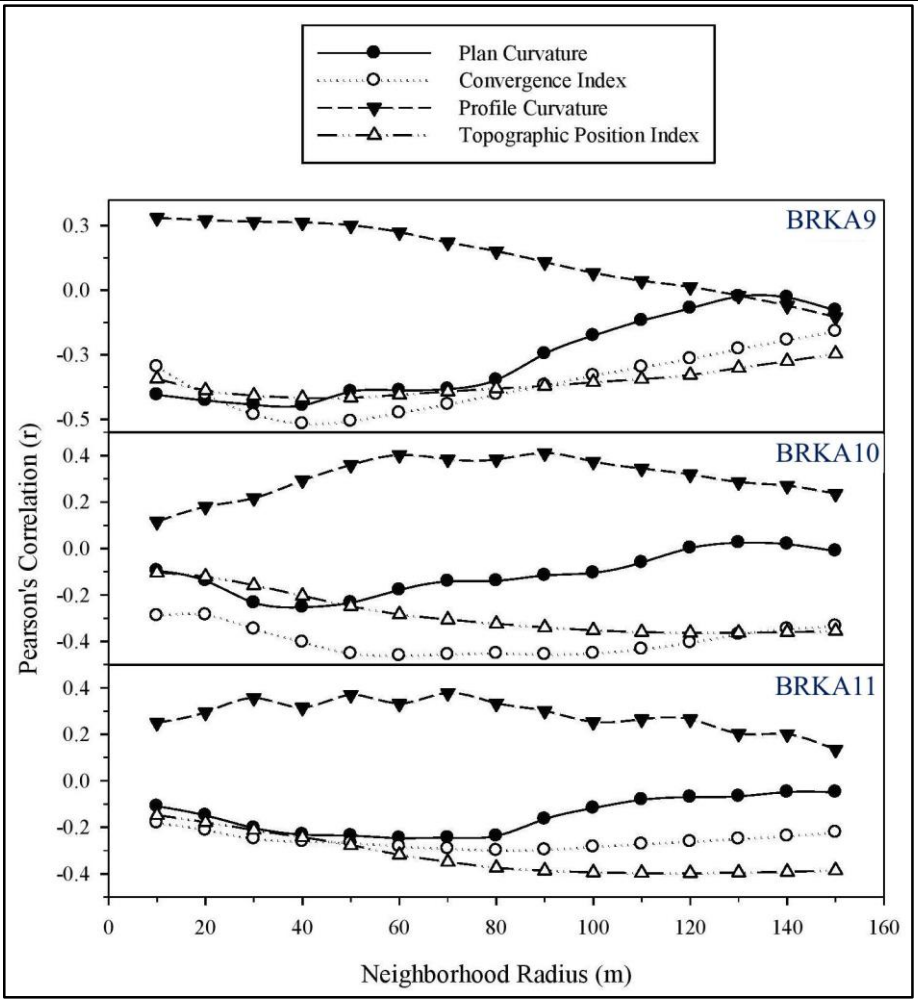

Figure 4. Pearson's correlation between soil phosphorus and terrain indices in BRKA9, BRKA10, and BRKA11 at neighborhood radiuses ranging from 10m to 150m.

Peak *r* for CI, profile curvature, and TPI occurred at larger NR at BRKA10 than at BRKA9. TPI (120 m) and profile curvature (90 m) NR were ≥ twice the NR of CI (60 m) and plan curvature (40 m) in BRAKA10, respectively, indicating that flow convergence/divergence influences soil P spatial distribution at smaller scales than flow acceleration/deceleration (Figure 5). Like BRKA9, CI ($r=-0.46$, $p<0.001$) was best correlated with soil P at BRKA10. Profile curvature ($r=0.41$, $p<0.05$) outperformed TPI ($r=-0.36$, $p<0.05$) while CI outperformed plan curvature ($r=-0.25$, $p>0.05$) whose correlation was non-significant.

Peak r for BRKA11 CI (80 m) and plan curvature (60 m) occurred at larger NR than in both BRKA9 and BRKA10. Further, peak r for profile curvature (50 m) occurred at a NR that was less than half the NR of TPI (120 m) peak *r* with soil P (Figure 5). Profile curvature ($r=0.37$, $p<0.05$) and TPI ($r=0.40$, $p<0.05$) were better correlated with soil P than both CI ($r=-0.30$, $p<0.05$) and plan curvature ($r=-0.25$, $p>0.05$), which suggests that the acceleration/deceleration of flow within BRKA11 controls soil P spatial distributions more so than flow convergence/divergence.

Journal of Geospatial Applications in Natural Resources Vol. 1, No. 1; 2016

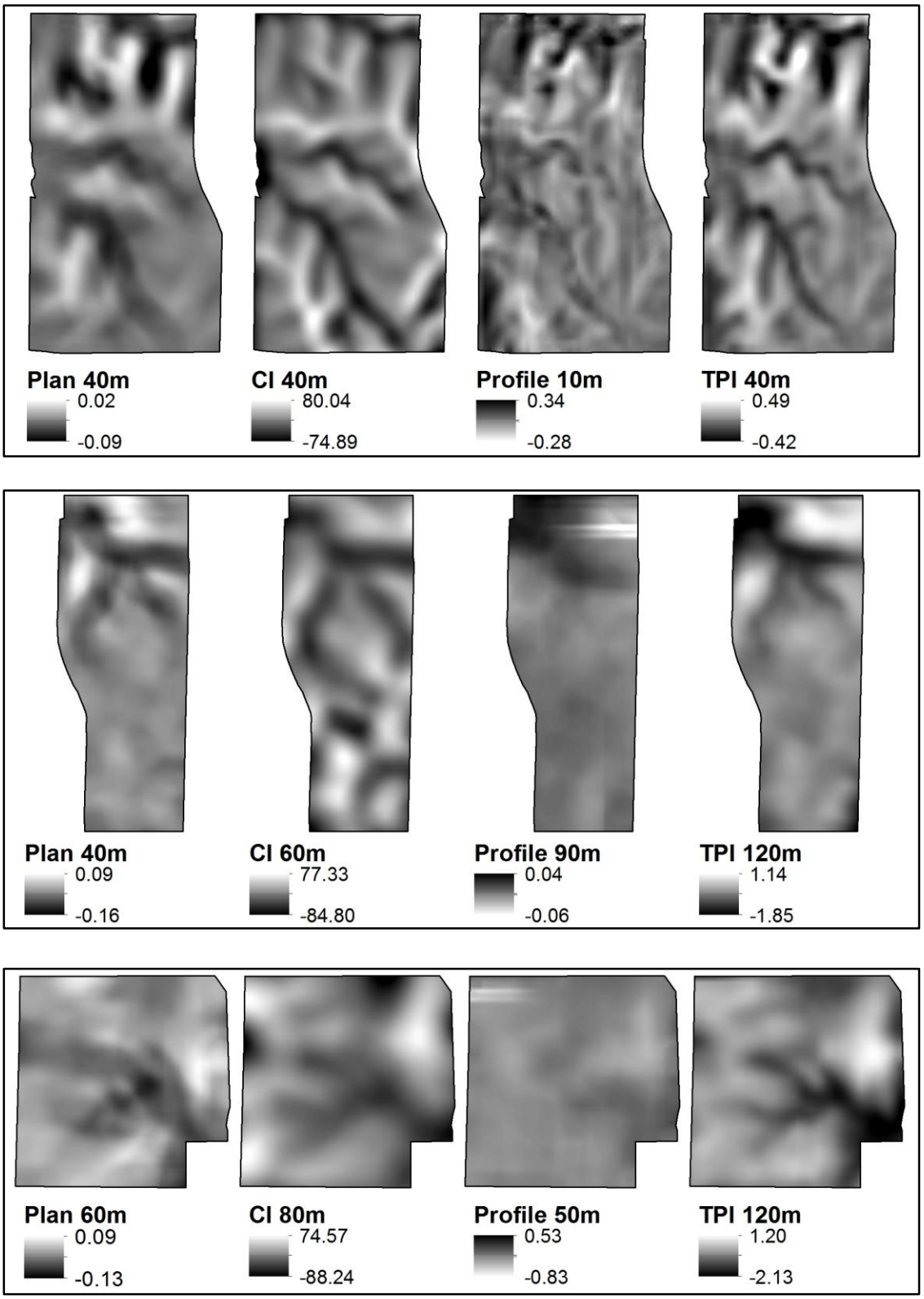

Figure 5. Terrain indices at the scale which correlation with soil phosphorus was greatest in BRKA9 (top), BRKA10 (middle), and BRKA11 (bottom).

The scales at which convergent/divergent indices and slope position indices best correlated with soil P represent the adequate area of a geomorphic characteristic (Florinsky and Kuryakova 2000). Where both convergent/divergent indices and slope position indices scales are found to be similar, convergent/divergent areas and slope positions will have the same adequate area; however, adequate areas of convergent/divergent areas and slope positions differ when the opposite is true. For instance, optimal TPI and CI scales are equal in BRKA9 and plan and profile curvatures are nearly equal in BRKA11. Therefore, the TPI method and Pennock method of landform classification will produce landforms whose adequate area parallel and perpendicular to the contour are equal in BRKA9 and BRKA11, respectively. When convergent/divergent indices scales are larger than slope position scales, the adequate area of convergence and divergence is less than the adequate area of hillslope facets which effectively reduces hillslope length compared to the distance between crests and valleys along the contour. This would be characteristic of landforms classified with the Pennock method in BRKA9. Alternatively, TPI scales are larger than CI scales in BRKA10 and BRKA11 while profile curvature scales were larger than plan curvature scales in BRKA10. Landforms classified with the TPI method in BRKA10 and BRKA11 and with the Pennock method in BRKA10 will produce landforms with greater slope lengths and more frequent undulation along the contour.

Landform Classifications

Landform classifications delinated using the TPI method are shown in Figure 6. Convergent footslopes in BRKA9, BRKA10, and BRKA11 were identified within grass waterways, flow accumulations, watershed outlets, and at the base of slopes. Divergent shoulders were located in local upland regions throughout each field. Level areas were mainly identified in upslope positions; although, level areas were also identified in the outlet where the southern and central grass waterway converge in BRKA9. Level areas within upslope positions are indicative of a summit whereas level areas at the bottom of slopes correspond to a toeslope. Further, convergent areas were identified within grass waterways and flow accumulations while divergent areas were identified in upslope positions. Therefore, >97% of all footslopes and shoulders were classified as convergent and divergent, respectively, in all three fields; however, convergent shoulders and divergent footslopes are typically uncommon in natural landscapes (Dragut and Blaschke 2006). Level areas comprised 46% of the total area of BRKA10 while level areas only comprised 13% and 1% of the total area of BRKA9 and BRKA11, respectively. This is reasonable because the level, upland area or summit in BRKA10 constitutes roughly half of its total area. A smaller percentage of the landforms were classified as level in BRKA 9 and BRKA11 because prominent ephemeral stream networks cut through these fields creating greater, local variability in elevation. Further, the total area of convergent and divergent landforms was nearly equal within BRKA9 and BRKA10, while BRKA11 had 15% more divergent than convergent landforms. This is because BRKA11 has the convergent, upslope positions that drain water to both the outlets in the northern and eastern edge of BRKA11 as well as those that drain water to the grass waterways in BRKA10. Linear slope positions constituted 16%, 41%, and 6% more of the total land area than concave and convex slope positions in BRKA9, BRKA10, and BRKA11, respectively, because of an extensive summit in the upland regions, gradual slopes that lead from upslope to downslope, and longer slope lengths.

Due to the subtle curvature of the landscape, the Pennock method classified 99% of BRKA9 and 100% of BRKA10 and BRKA11 as either level or convergent/divergent backslopes and failed to identify shoulders or footslopes within the study area. Level landforms were primarily located in upland regions or summits. Level areas also occurred

Journal of Geospatial Applications in Natural Resources Vol. 1, No. 1; 2016

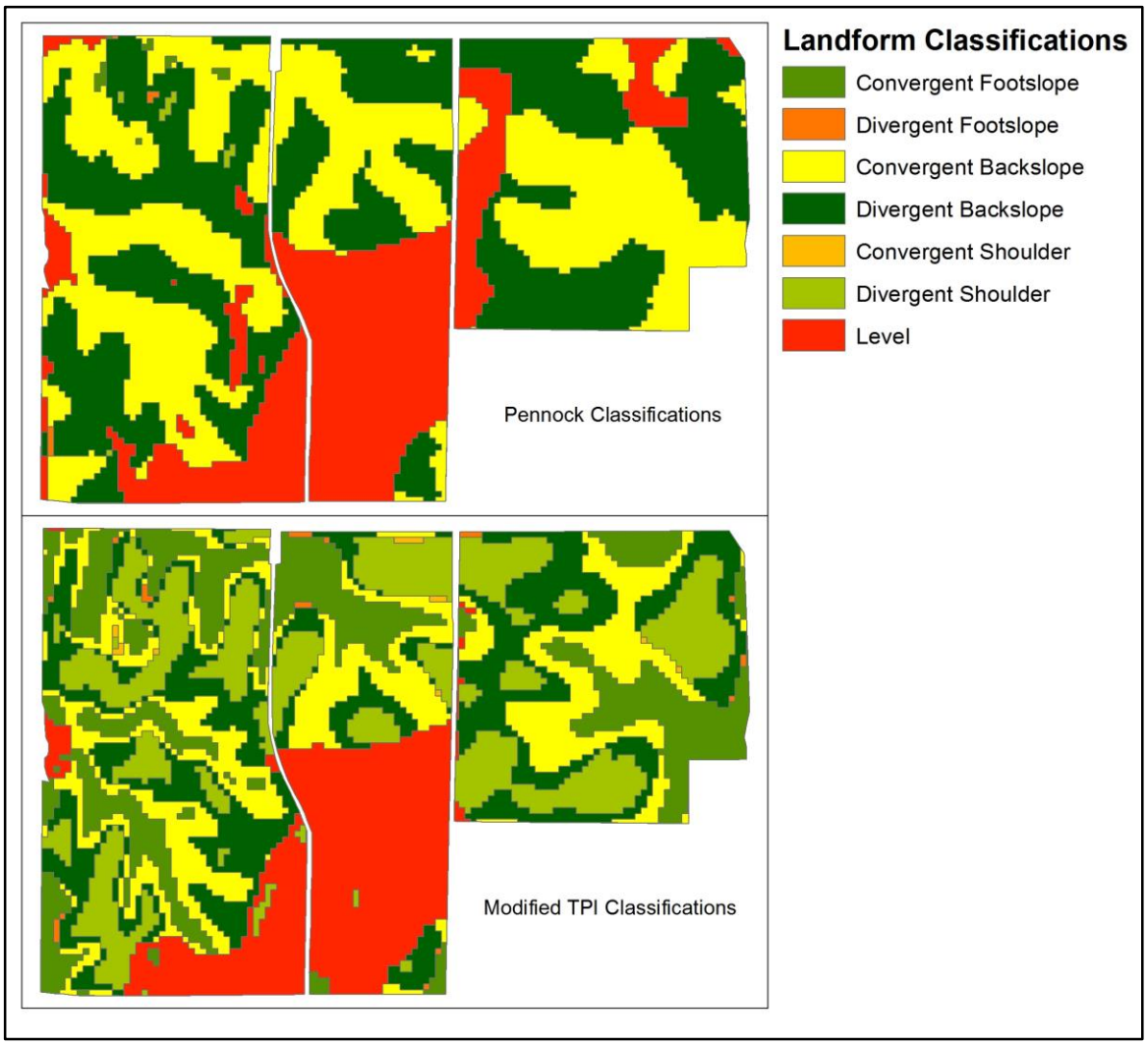

Figure 6. Landforms classified in BRKA9, BRKA10, and BRKA11 by the Pennock method (top) and the Modified TPI Classification method (bottom).

at all watershed outlets in BRKA9 as well as in a watershed outlet located on the northern edge of BRKA11. Convergent backslopes were located where flow accumulates and divergent backslopes were located in local upland regions. Similar to the TPI method, the Pennock method classified 46% of BRKA10 as level; however, the Pennock method classified 17% and 15% of BRAK9 and BRKA11, respectively, as level which is greater than the TPI classifications. Also, much more of the total area of all fields were classified as convergent/divergent backslopes compared to the TPI method classifications. Since the Pennock method failed to identify convergent footslopes and divergent shoulders, more area was left to be classified as either level or convergent/divergent backslopes. The Pennock method also classified nearly equal area as convergent and divergent landforms within BRKA9 and BRKA10, while BRKA11 had 5% more divergent than convergent landforms.

Significant differences of soil P on topographic positions classified with the modified TPI method were found in Table

2. Mean ± standard deviation soil phosphorus (P) on convergent footslopes (CF), convergent backslopes (CB), divergent backslopes (DB), divergent shoulders (DS), and level (L) landforms. Mean concentrations on landforms classified with the same method at the same field with different letters are significantly different (P<0.05).

Field	Method	CF	CB	DB	DS	L	R^2
		Soil P (mg kg^{-1})					
BRKA9	Pennock	NA	37.4±1.8b	33.3±2.3b	NA	64.7±7.3a	0.29
	Modified TPI	44.6±5.6a	36.6±2.4a	38.6±2.7a	24.1±2.4b	53.4±6.3a	0.3
BRKA10	Pennock	NA	66.6±6.3a	42.6±2.7b	NA	51.1±4.3ab	0.16
	Modified TPI	67.7±8.0a	61.7±8.3a	45.3±14.0a	42.8±3.0a	49.5±4.2a	0.16
BRKA11	Pennock	NA	34.6±2.4a	32.7±2.4a	NA	31.5±1.5a	0.01
	Modified TPI	49.5±6.8a	30.6±3.2b	35.3±1.8ab	29.1±2.3b	NA	0.19

BRKA9 and BRKA11 (Table 2). In BRKA9, divergent shoulders had significantly lower soil P than all other landforms indicating that erosion on shoulders is removing soil P and depositing it in downslope positions. Further, level areas in BRKA9 are most likely sinks of applied P since they contained the highest mean soil P. In BRKA11, convergent footslopes had significantly higher soil P than convergent backslopes and divergent shoulders. Convergent footslopes had the highest mean soil P among all landforms in both BRKA10 and BRKA11. Further, divergent backslopes had slightly higher soil P than convergent backslopes in BRKA9 and BRKA11.

Significant differences of soil P on topographic positions classified with the Pennock method were found in BRKA9 and BRKA10. Level areas had significantly higher soil P than divergent and convergent backslopes in BRKA9, while convergent backslopes had significantly higher soil P than divergent backslopes in BRKA10. As mentioned previously, level areas are most likely sinks of applied P; however, it is unclear why divergent backslopes have more soil P than convergent backslopes.

Both methods of landform classification explained similar amounts of variability in spatial soil P distribution in BRKA9 and BRKA10 while the modified TPI method outperformed the Pennock method in BRKA11. The Pennock method performed rather poorly in BRKA11 (R^2 = 0.01). Although soil P distribution throughout BRKA9, BRKA10, and BRKA11 are significantly correlated with topographic indices, the landforms delineated within these fields explain a low amount of the spatial variability of soil P ($R^2 \leq 0.30$). Therefore, landforms are not the sole factor driving spatial phosphorus variability. Soil P "hot spots" located at rill and watershed outlets may increase the varability of soil P within landforms. If certain landforms have better yields than others, then crop uptake will effect soil P spatial distribution. Also, soil P is most available at a pH of 6.5 which is within the pH range of the dominant soil series throughout the site, e.g. moderately acidic (pH 5.6-6.0) to neutral (pH 6.6 to 7.3); therefore, the spatial variability of pH could also affect the spatial variability of available soil P.

Conclusion

Two methods were compared that incorporated scale into landform modeling in low-relief agricultural fields. Soil P distribution and correlation analysis confirmed that slope, slope position, and convergence/divergence significantly influenced soil P distribution in all three study sites. The terrain indices derived to represent flow

convergence/divergence and acceleration/deceleration also influenced the characterization of soil P spatial distribution. In two of the three study sites, the TPI was better correlated to soil P than profile curvature while the CI was better correlated to soil P than plan curvature in all three sites. Therefore, the TPI and CI may be better alternatives to profile and plan curvature, respectively, when characterizing surface geometries in low-relief agricultural fields. The most appropriate scale found for each terrain indices was not constant between study sites, suggesting that surface geometries of each field were unique. The scale best suited for each terrain indices can also characterize the shape of the landscape, e.g. long/short slope length or frequent/occasional undulation along the contour. The main issue with the Pennock method was that it may fail to recognize concave and convex profile curvature features in low-relief agricultural fields. Although the Pennock method failed to identify footslopes and shoulders which are clearly part of these fields' topographic framework, this method delineated landforms that explained similar amounts of soil P variability as the TPI method in two of the three study sites. In flat plain landscapes with low-relief, the TPI and CI are suitable alternatives to plan and profile curvature for deriving convergent/divergent and slope position surface geometries. The TPI and CI should be further explored when performing terrain analysis at the agricultural field scale to create solutions for precision management objectives.

Acknowledgements

We would like to thank the Howard G. Buffett Foundation for their funding, time, and efforts that made this research possible. We would also like to thank Bryan Young and Laura Campbell for their help with the overall research project. Use of a company or product name does not imply approval or recommendation of the product by Southern Illinois University or the Howard G. Buffett Foundation.

References

Balkcom, K. S., Terra, J. A., Shaw, J. N., Reeves, D. W., & Raper, R. L. (2005). Soil management system and landscape position interactions on nutrient distribution in a Coastal Plain field. *Journal of Soil and Water Conservation*, 60, 431-437.

Brubaker, S. C., Jones, A. J., Frank, K., & Lewis, D. T. (1994). Regression models for estimating soil properties by landscape position. *Soil Science Society of America Journal*, 58, 1763-1767.

Brubaker, S. C., Jones, A. J., Lewis, D. T., & Frank, K. (1993). Soil properties associated with landscape position. *Soil Science Society of America Journal*, 57, 235-239.

Burrough, P. A., van Gaans, P. F. M., & Macmillan, R. A. (2000). High-resolution landform classification using fuzzy k-means. *Fuzzy Sets and Systems*, 113, 37-52.

Collman, R. D. (2009). *Soil Survey of Macon County, Illinois*. United States Department of Agriculture, Soil Conservation Service. U.S. Gov't Printing Off.

De Reu, J., Bourgeois, J., Bats, M., Zwertvaegher, A., Gelorini, V., De Smedt, P., Chu, W., Antrop, M., De Maeyer, P., Finke, P., Meirvenne, M. V., Verniers, J., & Crombe, P. (2013). Application of the topographic position index to heterogeneous landscapes. *Geomorphology*, 186, 39-49.

Deng, Y., Chen, X., Chuvieco, E., Warner, T., & Wilson, J. P. (2007). Multi-scale linkages between topographic attributes and vegetative indices in a mountainous landscape. *Remote Sensing of Environment*, 111, 122-134.

Deumlich, D., Schmidt, R., & Sommer, M. (2010). A multiscale soil-landform relationship in the glacial-drift area based on digital terrain analysis and soil attributes. *Journal of Plant Nutrition and Soil Science*, 173, 843-851.

Dikau, R. (1989). The application of a digital relief model to landform analysis in geomorphology. In J. Raper (Ed.), *Three dimensional applications in geographical information systems* (P. 51-78). UK: Taylor and Francis.

Dragut, L., & Blaschke, T. (2006). Automated classification of landform elements using object-based image analysis. *Geomorphology*, 81, 330-344.

Dragut, L., Schauppenlehner, T., Muhar, A., Strobl, J., and Blaschke, T. (2009). Optimization of scale and parameterization for terrain segmentation: An application to soil-landscape modeling. *Computers and Geoscience*, 35, 1875-1883.

Florinsky, I. V. (2012). *Digital terrain analysis in soil science and geology*. Boston: Elsevier/Academic Press.

Florinsky, I. V. and Kuryakova, G. A. (2000). Determination of grid size for digital terrain modeling in landscape investigations – exemplified by soil moisture distribution at a micro-scale. *International Journal of Geographical Information Science*, 14, 815-832.

GRASS Development Team. (2015). *GRASS GIS 7 Addons Manual*. Retrieved from http://grass.osgeo.org/grass70/manuals/addons/r.convergence.html.

Hansen, N. C., Daniel, T. C., Sharpley, A. N., and Lemunyon, J. L. (2002). The fate and transport of phosphorus in agricultural systems. *Journal of Soil and Water Conservation*, 57, 408-417.

Havlin, J. L., Beaton, J. D., Tisdale, S. L., and Nelson, W. L. (2005). *Soil fertility and fertilizers: an introduction to nutrient management* (21st ed.). Upper Saddle River, New Jersey: Pearson Prentice Hall.

Hawley, M. E., Jackson, T. J., and McCuen, R. H. (1983). Surface soil moisture variation on small agricultural watersheds. *Journal of Hydrology*, 62, 179-200.

Jenness, J. (2006). *Topographic Position Index (tpi_jen.avx) extension for ArcView 3.x, v.1.3a*. Retrieved from http://www.jennessent.com/arcview/tpi.htm.

Kirkby, M. J. and Chorley, R. J. (1967). Throughflow, overland flow, and erosion. *International Association of Scientific Hydrology Bulletin*, 12, 5-21.

Kravchenko, A. N. and Bullock, D. G. (2000). Correlation of corn and soybean grain yield with topography and soil properties. *Agronomy Journal*, 92, 75-83.

Malo, D. D. and Worcester, B. K. (1974). Soil fertility and crop responses at selected landscape positions. *Agronomy Journal*, 67, 397-401.

Mehlich, A. (1984). Mehlich-3 soil test extractant: A modification of Mehlich-2 extractant. *Communications in Soil Science and Plant Analysis*, 15, 1409-1416.

Needelman, B. A., Gburek, W. J., Peterson, G. W., Sharpley, A. N., and Kleinman, P. J. A. (2004). Surface runoff along two agricultural hillslopes with contrasting soils. *Soil Science Society of America Journal*, 68, 914-923.

Pimentel, D. (2000). Soil erosion and the threat to food security and the environment. *Ecosystem Health*, 6, 221-226.

Pennock, D. J., Zebarth, B. J., and De Jong, E. (1987). Landform classification and soil distribution in hummocky terrain, Saskatchewan, Canada. *Geoderma*, 40, 297-315.

Schmitt, J. and Hewitt, A. (2004). Fuzzy land element classification from DTMs based on geometry and terrain position. *Geoderma*, 121, 243-256.

Shi, X., Zhu, A. X., Burt, J., Choi, W., Wang, R., Pei, T., Li, B., and Qin, C. (2007). An experiment using a circular neighborhood to calculate slope gradient from a DEM. *Photogrammetric Engineering & Remote Sensing*, 73, 143-154.

Soil Survey Staff, Natural Resources Conservation Service, United States Department of Agriculture. *Official Soil Series Descriptions*. Retrieved from https://soilseries.sc.egov.usda.gov/osdname.asp.

Soon, Y. K. and Malhi, S. S. (2005). Soil nitrogen dynamics as affected by landscape position and nitrogen fertilizer. *Canadian Journal of Soil Science*, 85, 579-587.

Thommeret, N., Bailly, J. S., and Puech, C. (2010). Extraction of thalweg networks from DTMs: application to badlands. *Hydrology and Earth System Sciences*, 14, 1527-1536.

Weiss, A. (2001). *Topographic Position and Landform Analysis*. San Diego, CA: Poster presentation, ESRI User Conference.

Wood, J. (1996). *The geomorphological characterization of digital elevation models* (PhD Thesis). Department of Geography, University of Leicester, UK.